

Are Starburst Galaxies Proton Calorimeters?

Xilu Wang* and Brian D. Fields

University of Illinois at Urbana-Champaign, USA

E-mail: xwang107@illinois.edu, bdfields@illinois.edu

In star-forming galaxies, gamma rays are mainly produced through the collision of high-energy protons in cosmic rays and protons in the interstellar medium (i.e., cosmic-ray induced π^0 γ -radiation). For a “normal” star-forming galaxy like the Milky Way, most cosmic rays escape the galaxy before such collisions, but in starburst galaxies with dense gas and huge star formation rate, it is thought that most cosmic rays “die” in these interactions. To test this, we construct a “thick-target” model for the starburst galaxies, in which cosmic rays are accelerated by supernovae, and escape is neglected. This model gives an upper limit to a galaxy’s gamma-ray emission, and tests the calorimetric relation between gamma rays and cosmic rays for starbursts. Only two free parameters are involved in the model: the cosmic-ray proton acceleration energy per supernova ϵ_{cr} , and the proton injection spectral index s . We apply our model to five observed starburst galaxies: M82, NGC 253, NGC 1068, NGC 4945 and the Circinus galaxy, and find most of these starbursts are consistent with being proton calorimeters, with $\epsilon_{\text{cr}} \sim (0.1 - 0.25) \times 10^{51}$ erg and $s \sim 2.1 - 2.4$. But we confirm that for Circinus, other gamma-ray sources are needed to explain its GeV luminosity.

*The 34th International Cosmic Ray Conference,
30 July- 6 August, 2015
The Hague, The Netherlands*

*Speaker.

1. Introduction

Cosmic rays (CRs) are accelerated by supernova explosions (e.g., [1, 2, 3]), and thus cosmic rays should be present in all galaxies hosting supernovae. As CRs propagate in the interstellar medium (ISM), inelastic collisions between CR and interstellar nuclei—both dominantly protons—yield pionic gamma rays via $p_{\text{cr}}p_{\text{ism}} \rightarrow pp\pi^0, \pi^0 \rightarrow \gamma\gamma$ [4, 5]. This hadronic process occurs in the Milky Way, but should also in other star-forming galaxies (e.g., [6, 7, 8, 9, 10, 11]). *Fermi*-LAT is the first GeV gamma-ray telescope to study external star-forming galaxies as a population. *Fermi* has detected three ordinary external star-forming galaxies: the Large Magellanic Cloud (LMC [12]), the Small Magellanic Cloud (SMC [13]) and M31 [14]. *Fermi* also detects five starburst galaxies: M82 and NGC253 [15], NGC4945 and NGC1068 [16], as well as the Circinus galaxy [17]. The two nearest and brightest starbursts, M82 and NGC253, are also detected at TeV energies by *VERITAS* [18] and *H.E.S.S.* [19, 20], respectively.

Starburst galaxies are a particularly interesting class of star-forming galaxies. Compared with normal galaxies like Milky Way, starbursts have exceptionally high star-formation rates and harbor regions of very dense gas. Thus cosmic rays accelerated in starbursts are expected to “die” in collisions with ISM rather than escape. In the limit where all the CR nuclei interact with ISM, a large fraction of proton energy is emitted as gamma rays, making such a galaxy a “proton calorimeter” (e.g., [21, 22, 20]). This situation has the maximum efficiency to convert supernova blast energy into gamma rays.

Our aim is to self-consistently calculate the pionic emission from starbursts in a closed box, and to use starburst data to test this calorimetric scenario. Existing models for nonthermal particles in starbursts have included both hadronic and leptonic processes such as synchrotron radiation, inverse Compton scattering and pion production (e.g., [23, 24, 22, 25]). Many—but not all—of these models predict that hadronic processes dominate above a few GeV. By construction, our more focused model is economical and thus easy to test: it contains only two parameters, the cosmic-ray acceleration energy per supernova ϵ_{cr} , and the cosmic-ray injection index s . The next section will briefly introduce the model. Results are presented in section 3. In section 4, further discussions and conclusions are given. For detailed model construction and results, see [26].

2. Theoretical model: the Thick-Target/Calorimetric Model

Our model is a thick-target “closed-box” model which has the following basic assumptions: 1) cosmic-rays and ISM particles distributions are spatially homogeneous (one zone); 2) cosmic-rays are initially accelerated by supernovae (SN) with acceleration energy per SN ϵ_{cr} ; 3) the injected cosmic-ray/proton spectrum is a power law in momentum, of spectral index s in GeV and TeV energy range; 4) all the cosmic rays will interact with ISM, i.e., the escape rate of protons is zero; 5) among the gamma-ray production mechanisms, pion production and decay dominates.

We adopt an injected cosmic-ray spectrum is $q_p \equiv dq/dp = dN_p/dV dt dE \propto p^{-s}$, with p is the proton momentum, and the free parameter $s > 2$ is the proton injection index. Thus the cosmic ray injected power, i.e., luminosity $dE_{\text{cr}}/dt = L_{\text{cr}} = \int E q_p dp dV$. Let cosmic rays be accelerated by supernovae that explode at a rate R_{sn} . Then the normalization of q_p is fixed via energy conservation:

$L_{\text{cr}} = \varepsilon_{\text{cr}} R_{\text{sn}}$, which gives $q_p \propto \varepsilon_{\text{cr}} R_{\text{sn}} p^{-s}$. Here ε_{cr} is the mean energy per SN going into CRs. This is our other free parameter.

We describe cosmic-ray propagation (e.g., [27]) with a one-zone, closed-box, equilibrium model. Losses are only due to cosmic-ray interactions with ISM, and omit escape. Considering the elastic [28] and ionic energy loss rate [2], energy loss (per nucleon) per time is $b(n_{\text{gas}}, E_p) = -dE/dt = b_{\text{inelastic}} + b_{\text{elastic}} + b_{\text{ionic}}$, E_p is the total energy of proton, n_{gas} is the atomic hydrogen density of ISM. This fixes the calorimetric propagated proton flux to be:

$$\phi_p(E) = \frac{dN_p}{dAdtdE} = \frac{v_p}{b(n_{\text{gas}}, E_p)} \int_{E_p}^{\infty} q_p(E) dE \propto \varepsilon_{\text{cr}} R_{\text{sn}} I(> E_p, s) \quad (2.1)$$

where v_p is the velocity of proton, I is here a function of E_p and s .

Adopting ref. [5]’s approach in getting π^0 productions’ differential cross-section, we can calculate $b_{\text{inelastic}}$ self-consistently. And using the pion spectrum q_π and gamma-ray spectrum q_γ equations, our model’s gamma-ray number flux from a starburst galaxy is:

$$F_\gamma = \frac{dN_{\gamma, \text{observed}}}{dE_\gamma dAdt} = \mathcal{A} \cdot \frac{1}{4\pi d^2} \cdot \frac{dN_\gamma(E_\gamma; \varepsilon_{\text{cr}}, s)}{dE_\gamma} \cdot R_{\text{sn}} \quad (2.2)$$

where d is the distance of the galaxy, E_γ is the total energy of photon. The gamma-ray flux is an observable from *Fermi*. $N_{\gamma, \text{observed}}$ is the gamma-ray number measured by the telescope. The galaxy’s “effective” gamma-ray number yield per supernova N_γ (gamma-rays are indirectly created by supernovae) is calculated in our model ($N_\gamma \propto \varepsilon_{\text{cr}}$). The total gamma ray production rate is the production of N_γ and R_{sn} . To account for the contribution from particle interactions involving nuclei with atomic weights $A > 1$ in both CRs and ISM, a nuclear enhancement factor of $\mathcal{A} = 0.59$ is included in the calculation [26].

We can see that, for a certain starburst galaxy, our model’s gamma-radiation results only depend on two parameters: cosmic-ray proton acceleration energy per supernova ε_{cr} (direct proportionality) and the injected proton spectral index s . So we only need to vary the two parameters ε_{cr} and s to find the best fit of the model to observed data by Chi-squared test.

3. Results

3.1 Individual Starbursts

We apply our thick-target, closed-box model to five starbursts with GeV data. For each galaxy we adopt/infer an observed star-formation rate (SFR), and then calculate the pionic flux $E_\gamma^2 dN_{\pi \rightarrow \gamma\gamma} / dE_\gamma dAdt$ as in $(\varepsilon_{\text{cr}}, s)$ space. We perform χ^2 test with the observed gamma-ray data to get the best-fit model parameters, which appear in Table 1, with ε_{cr} in units of $1\text{foe} \equiv 10^{51}\text{erg} \equiv 1\text{Bethe}$.

We plot the best-fit pionic gamma-ray spectra of NGC253 and Circinus in Figure 1. These cases bracket the extremes, and illustrate general features of our model spectra: (1) the shape only depends on the injected proton spectrum; (2) the magnitude is proportional to ε_{cr} ; (3) at high energies, the gamma-ray spectral index is the same as the proton injection index s , and is flatter than in the escape-dominated galaxies; (4) the peak energy is insensitive to s , and corresponds to the “pion-bump” feature [4, 5]. For NGC253, we see that our best fit to GeV and TeV data is quite

Galaxy Name	SN Rate R_{SN} [century $^{-1}$]	CR source index \hat{s}	CR acceleration energy per SN ϵ_{cr} [foe/SN]	Γ^{Fermi}	GeV data reference	TeV data reference
M82	5.7 ± 0.9	2.275 ± 0.102	0.106 ± 0.025	2.25 ± 0.13 [29]	[18]	
NGC253	2.6 ± 0.4	2.350 ± 0.037	0.116 ± 0.013	2.18 ± 0.09	[30]	[20]
NGC4945	3.2 ± 0.9	2.400 ± 0.446	$0.210 (> 0.103)$	2.05 ± 0.13	[29]	
NGC1068	35 ± 9	2.100 ± 0.617	$0.253 (> 0.128)$	2.29 ± 0.19	[29]	[31]
Circinus	1.9 ± 0.5	2.300 ± 0.486	$0.619 (> 0.310)$	2.19 ± 0.12	[17]	

Table 1: Results and parameters set for the starbursts in the ‘‘Thick-Target’’ Model. *Fermi* power-law fits for the gamma data of starbursts are from ref. [17] with $dN/dE \propto E^{-\Gamma}$.

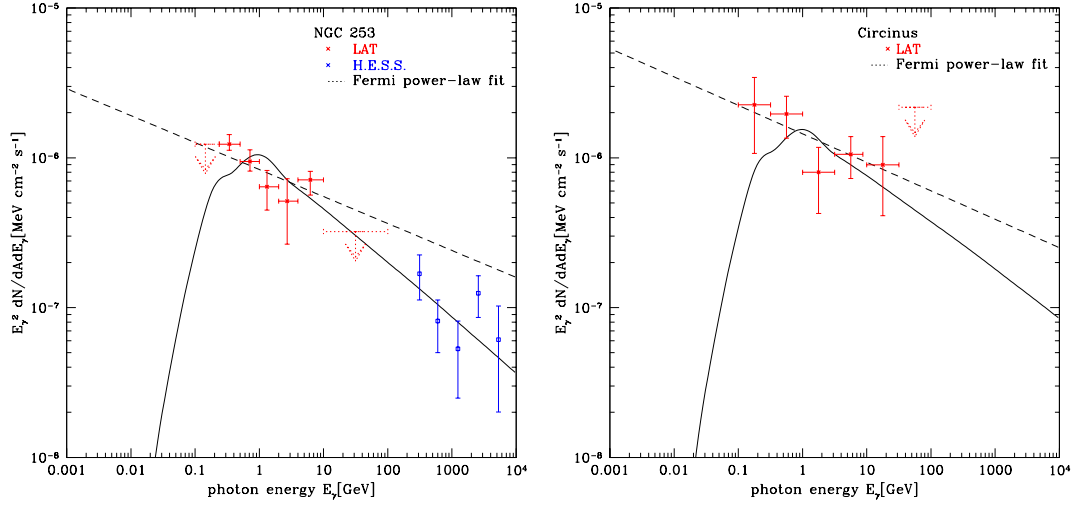


Figure 1: Left panel: Differential pionic gamma-ray spectrum (solid curve) for NGC253 with the best-fit parameters: source CR index s and accelerated CR energy per SN ϵ_{cr} . *Fermi* points are stars (red), *H.E.S.S.* points are squares (blue), and black dotted line is *Fermi*’s power-law fit to GeV data. References see Table 1. Right panel: Similar spectrum for Circinus.

good and fairly well constrained thanks to the relatively large energy range. For Circinus, only GeV data is available and even our simple model is poorly constrained.

For all starbursts, χ^2 contours appear in Figure 2. Both NGC253 and M82 have TeV data and good GeV data, and thus both s and ϵ_{cr} are well-constrained. For these galaxies, we find $\epsilon_{\text{cr}} \sim 0.10$ foe, in good agreement with canonical estimates for Milky Way cosmic rays [2]. For NGC1068, NGC4945 and Circinus, lack of TeV data leaves the parameters poorly constrained, with large uncertainties in *both* ϵ_{cr} and s . For these galaxies, Table 1 thus reports the *minimum* ϵ_{cr} consistent with the data.

We adopt a *maximum* value of $\epsilon_{\text{cr,max}} = 0.3\text{foe}$ in order to judge the proton calorimetry of the starbursts: if $\epsilon_{\text{cr}} < \epsilon_{\text{cr,max}}$, the starburst is a proton calorimeter with the calorimetric efficiency to be $\epsilon_{\text{cr}}/\epsilon_{\text{cr,max}}$, i.e., M82 has a calorimetric efficiency of 35%, NGC253 is 39%, NGC1068 is 84% and NGC4945 is 70%; if $\epsilon_{\text{cr}} > \epsilon_{\text{cr,max}}$, calorimetry fails for that galaxy as our model gives an upper-limit to the gamma-ray spectrum, other dominant gamma-ray sources must exist (e.g., AGNs) to explain the gamma-ray signal, therefore the Circinus galaxy is not a proton calorimeter.

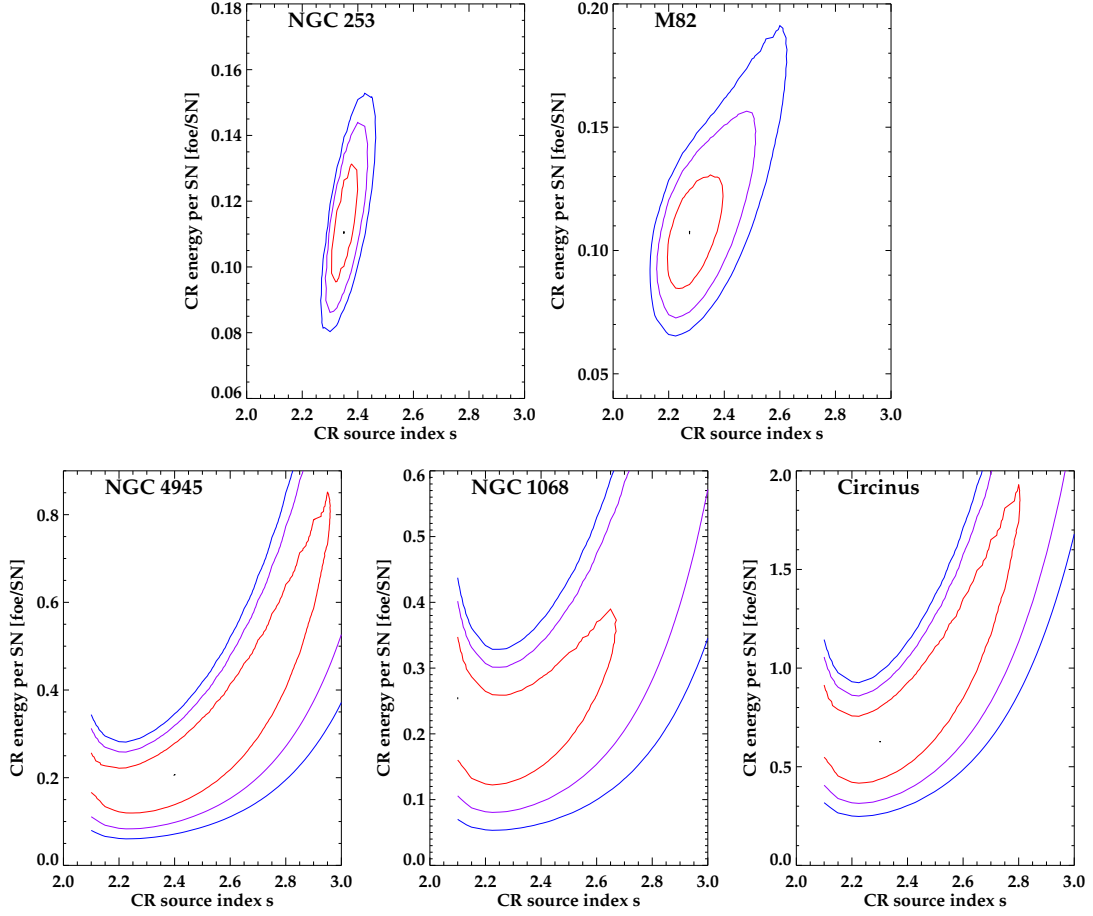


Figure 2: Contour plots for the χ^2 test of five starburst galaxies: best-fit value is the black dot; (red, magenta, blue) lines represent (70% CL, 95% CL, 99% CL). Above: Starbursts with well-constrained CR parameters s and ϵ_{cr} (has TeV data). Below: Starbursts with less-constrained CR s and ϵ_{cr} (lack of TeV data).

3.2 Calorimetric Limit

In a calorimeter case (again taken to be $\epsilon_{\text{cr,max}} = 0.3\text{foe}$), eq. 2.2 gives $F_\gamma \propto R_{\text{SN}} \propto \text{SFR } \psi$, therefore L_γ/ψ depends only on s . Using far-IR luminosity as a proxy for ψ , the expected calorimetric limit ratio $L_{>1\text{GeV}}/L_{8-100\mu\text{m}} = 5.2 \times 10^{-4}$ in our model with $s = 2.0$. Ref. [22] calculated the ratio to be 3.1×10^{-4} while *Fermi* group’s result is 2.5×10^{-4} [29].

The gamma-ray over far-IR luminosity ratio $L_{0.1-100\text{GeV}}/L_{8-100\mu\text{m}}$ expected in the calorimetric limit for CR nuclei is plotted in Fig 3. Our calorimetric limits agree with *Fermi* group’s [29] result within 30%, with different choices of the CR proton index s . Normal star-forming galaxies are about an order of magnitude below the calorimetric limits; starburst galaxies M82, NGC253, NGC1068 and NGC4945 are close to the limits, showing that good calorimetry relations hold for these galaxies, and starbursts have higher calorimetric efficiency than normal galaxies. The Circinus galaxy lies well above the limits, indicating other gamma-ray sources dominate.

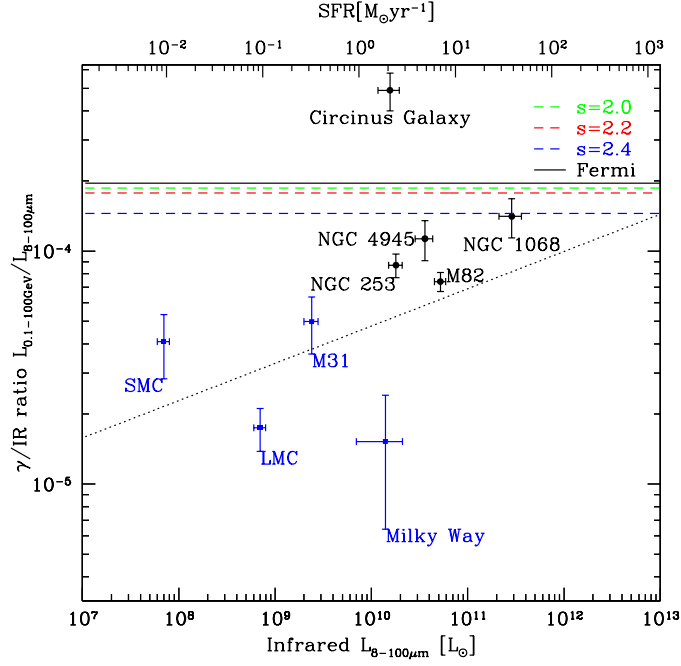


Figure 3: Plot of ratio of gamma-ray luminosity (0.1-100GeV) to total IR luminosity (8-100 μ m). Star-forming galaxies are indicated with blue squares (IR and gamma-ray data of the Milky Way is calculated from [11], IR data for other galaxies is from [32], gamma-ray data for SMC is from [13], LMC is from [12], M31 is from [14]). Starburst galaxies are marked with black dots (IR data is from [33], gamma-ray data is from [29], except for Circinus [17]). The black dotted line is *Fermi*'s best-fit power law relation [29]. The upper abscissa indicates SFR estimated from the IR luminosity according to the Kennicutt relation [34]. The colored dashed lines represents the expected gamma-ray luminosity in the calorimetric limit assuming an average CR acceleration energy per supernova of $\epsilon_{\text{cr}} = 0.3\text{foe}$ with various source CR index $s = 2.0, 2.2, 2.4$. The black solid line indicates *Fermi*'s calorimetric result ($s = 2.2, \epsilon_{\text{cr}} = 0.1\text{foe}$) [29].

4. Discussion

In this paper, we construct a two-parameter, closed-box, thick-target model to test the cosmic-ray calorimetry in starburst galaxies. For the best-measured starbursts, our model gives good fits to the gamma-ray data in both GeV and TeV range with s and ϵ_{cr} values consistent with those of Galactic cosmic rays. The goodness of our fit to starbursts M82, NGC253, NGC1068 and NGC4945 suggests that starburst galaxies are proton calorimeters with various calorimetric efficiencies. These efficiencies may be different in reality if the actual supernova acceleration of CR rate in starbursts differs from the calorimeter value $\epsilon_{\text{cr,max}} = 0.3\text{foe}$ adopted. For the Circinus galaxy, our model's gamma-ray over-luminosity result agrees with ref. [17], indicating additional gamma-ray sources are needed to explain the observed data.

However, more data is needed to fill in the energy gap to do a further check of our model's results. There is a lack of data at energy $\sim 30\text{-}100$ MeV for the starburst galaxies, so it is difficult to tell whether the actual gamma-radiation has the characteristic "pion bump". TeV data for NGC1068, NGC4945 and Circinus is also needed to constrain the choices of parameters (both s and ϵ_{cr}) in our model with smaller uncertainty. Moreover, recent *NuStar* X-ray limits on NGC253

in the 7-20 keV band disfavors leptonic processes dominating in the GeV and TeV energy range [35].

Acknowledgments

We are pleased to thank Keith Bechtol for providing *Fermi* data, Wystan Benbow for *VERITAS* data. XW thanks the ICRC organizers for financial support, and for an enjoyable conference. This work was supported in part by the NASA ATP through award NNX10AC86G.

References

- [1] W. Baade and F. Zwicky, *Cosmic Rays from Super-novae, Proceedings of the National Academy of Science* **20** (May, 1934) 259–263.
- [2] V. L. Ginzburg and S. I. Syrovatskii, *The Origin of Cosmic Rays*. Macmillan, New York, 1964.
- [3] F. Ackermann, M. et al., *Detection of the Characteristic Pion-Decay Signature in Supernova Remnants, Science* **339** (Feb., 2013) 807–811, [[arXiv:1302.3307](#)].
- [4] F. W. Stecker, *Cosmic gamma rays, NASA Special Publication* **249** (1971).
- [5] C. D. Dermer, *Secondary production of neutral pi-mesons and the diffuse galactic gamma radiation, A&A* **157** (Mar., 1986) 223–229.
- [6] A. W. Strong, A. W. Wolfendale, and D. M. Worrall, *Origin of the diffuse gamma ray background, MNRAS* **175** (May, 1976) 23P–27P.
- [7] G. G. Lichti, G. F. Bignami, and J. A. Paul, *The gamma-ray luminosity of spiral galaxies - Its evolution and its contribution to the diffuse background above 100 MeV, ApSS* **56** (July, 1978) 403–414.
- [8] V. Pavlidou and B. D. Fields, *Diffuse Gamma Rays from Local Group Galaxies, ApJ* **558** (Sept., 2001) 63–71, [[astro-ph/0105207](#)].
- [9] F. W. Stecker and T. M. Venters, *Components of the Extragalactic Gamma-ray Background, ApJ* **736** (July, 2011) 40, [[arXiv:1012.3678](#)].
- [10] A. A. Abdo and Fermi LAT Collaboration, *Fermi Large Area Telescope Measurements of the Diffuse Gamma-Ray Emission at Intermediate Galactic Latitudes, Physical Review Letters* **103** (Dec., 2009) 251101, [[arXiv:0912.0973](#)].
- [11] A. W. Strong and T. A. Porter, et al., *Global Cosmic-ray-related Luminosity and Energy Budget of the Milky Way, ApJL* **722** (Oct., 2010) L58–L63, [[arXiv:1008.4330](#)].
- [12] A. A. Abdo and M. Ackermann, et al., *Observations of the Large Magellanic Cloud with Fermi, A&A* **512** (Mar., 2010) A7.
- [13] A. A. Abdo and M. Ackermann, et al., *Detection of the Small Magellanic Cloud in gamma-rays with Fermi/LAT, A&A* **523** (Nov., 2010) A46.
- [14] A. A. Abdo and M. Ackermann, et al., *Fermi Large Area Telescope observations of Local Group galaxies: detection of M 31 and search for M 33, A&A* **523** (Nov., 2010) L2, [[arXiv:1012.1952](#)].
- [15] A. A. Abdo and Fermi LAT Collaboration, *Detection of Gamma-Ray Emission from the Starburst Galaxies M82 and NGC 253 with the Large Area Telescope on Fermi, ApJL* **709** (Feb., 2010) L152–L157, [[arXiv:0911.5327](#)].

- [16] P. L. Nolan and A. A. Abdo, et al., *Fermi Large Area Telescope Second Source Catalog*, *ApJS* **199** (Apr., 2012) 31, [[arXiv:1108.1435](#)].
- [17] M. Hayashida and Ł. Stawarz, et al., *Discovery of GeV Emission from the Circinus Galaxy with the Fermi Large Area Telescope*, *ApJ* **779** (Dec., 2013) 131, [[arXiv:1310.1913](#)].
- [18] V. A. Acciari and VERITAS Collaboration, *A connection between star formation activity and cosmic rays in the starburst galaxy M82*, *Nature* **462** (Dec., 2009) 770–772, [[arXiv:0911.0873](#)].
- [19] F. Acero and F. Aharonian, et al., *Detection of Gamma Rays from a Starburst Galaxy*, *Science* **326** (Nov., 2009) 1080–, [[arXiv:0909.4651](#)].
- [20] A. Abramowski and H. E. S. S. Collaboration, *Spectral Analysis and Interpretation of the γ -Ray Emission from the Starburst Galaxy NGC 253*, *ApJ* **757** (Oct., 2012) 158, [[arXiv:1205.5485](#)].
- [21] M. Pohl, *On the predictive power of the minimum energy condition. I - Isotropic steady-state configurations*, *A&A* **270** (Mar., 1993) 91–101.
- [22] B. C. Lacki and T. A. Thompson, et al., *On the GeV and TeV Detections of the Starburst Galaxies M82 and NGC 253*, *ApJ* **734** (June, 2011) 107, [[arXiv:1003.3257](#)].
- [23] M. Persic, Y. Rephaeli, and Y. Arieli, *Very-high-energy emission from M 82*, *A&A* **486** (July, 2008) 143–149.
- [24] E. de Cea del Pozo, D. F. Torres, and A. Y. Rodriguez Marrero, *Multimessenger Model for the Starburst Galaxy M82*, *ApJ* **698** (June, 2009) 1054–1060, [[arXiv:0901.2688](#)].
- [25] T. M. Yoast-Hull and J. E. Everett, et al., *Winds, Clumps, and Interacting Cosmic Rays in M82*, *ApJ* **768** (May, 2013) 53, [[arXiv:1303.4305](#)].
- [26] X. Wang and B. D. Fields, *Are Starburst Galaxies Proton Calorimeters? in preparation, 2015, .*
- [27] M. Meneguzzi, J. Audouze, and H. Reeves, *The production of the elements Li, Be, B by galactic cosmic rays in space and its relation with stellar observations.*, *A&A* **15** (1971) 337–359.
- [28] R. J. Gould, *Effects of nuclear forces on ion thermalization in high-temperature plasmas*, *ApJ* **263** (Dec., 1982) 879–890.
- [29] M. Ackermann and M. Ajello, et al., *GeV Observations of Star-forming Galaxies with the Fermi Large Area Telescope*, *ApJ* **755** (Aug., 2012) 164, [[arXiv:1206.1346](#)].
- [30] T. A. D. Paglione and R. D. Abrahams, *Properties of nearby Starburst Galaxies Based on their Diffuse Gamma-Ray Emission*, *ApJ* **755** (Aug., 2012) 106, [[arXiv:1206.3530](#)].
- [31] F. Aharonian and A. G. Akhperjanian, et al., *Observations of selected AGN with HESS*, *A&A* **441** (Oct., 2005) 465–472, [[astro-ph/0507207](#)].
- [32] D. B. Sanders and J. M. Mazzarella, et al., *The IRAS Revised Bright Galaxy Sample*, *The Astronomical Journal* **126** (Oct., 2003) 1607–1664, [[astro-ph/0306263](#)].
- [33] Y. Gao and P. M. Solomon, *The Star Formation Rate and Dense Molecular Gas in Galaxies*, *ApJ* **606** (May, 2004) 271–290, [[astro-ph/0310339](#)].
- [34] R. C. Kennicutt, Jr., *The Global Schmidt Law in Star-forming Galaxies*, *ApJ* **498** (May, 1998) 541–552, [[astro-ph/9712213](#)].
- [35] D. R. Wik and B. D. Lehmer, et al., *Spatially Resolving a Starburst Galaxy at Hard X-Ray Energies: NuSTAR, Chandra, and VLBA Observations of NGC 253*, *ApJ* **797** (Dec., 2014) 79, [[arXiv:1411.1089](#)].